

Supplementary Materials for

Charge-switchable polymeric complex for glucose-responsive insulin delivery in mice and pigs

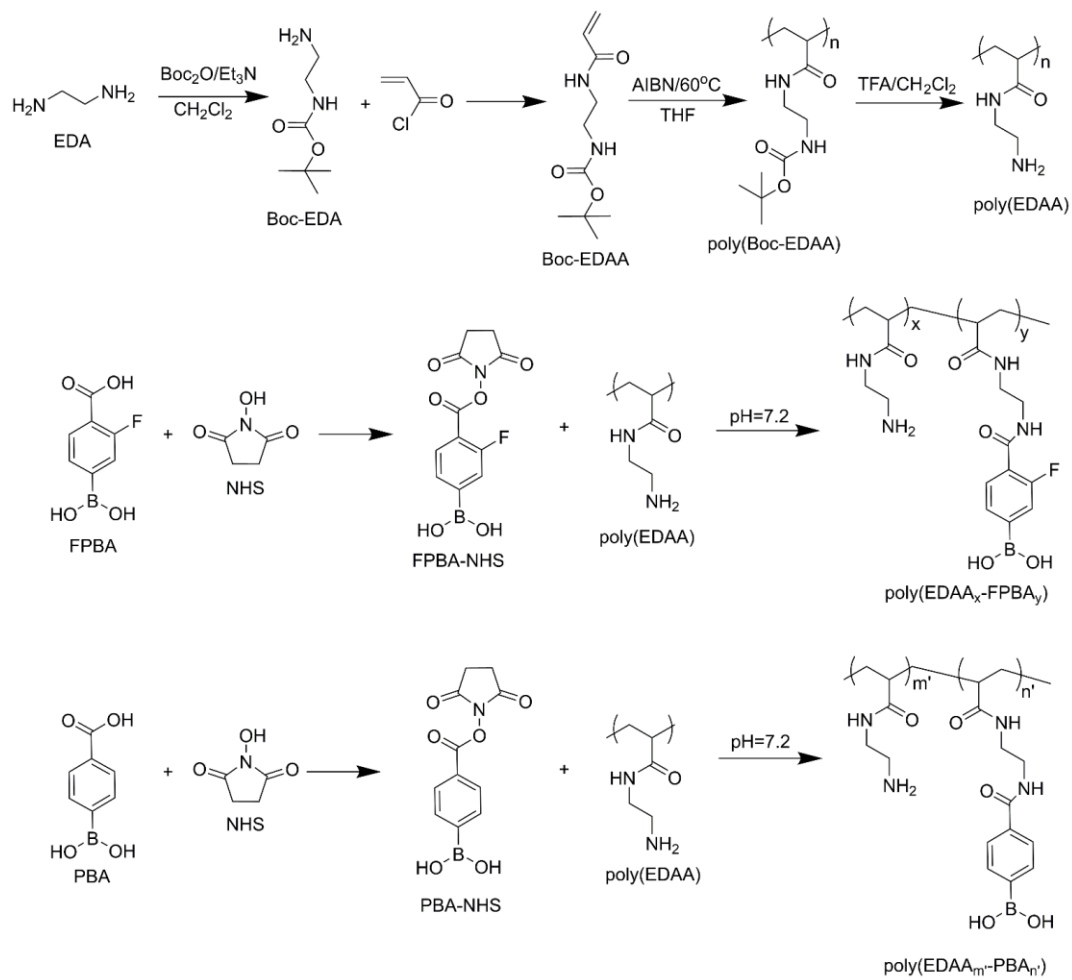
Jinqiang Wang, Jicheng Yu, Yuqi Zhang, Xudong Zhang, Anna R. Kahkoska, Guojun Chen, Zejun Wang, Wujin Sun, Lulu Cai, Zhaowei Chen, Chenggen Qian, Qundong Shen, Ali Khademhosseini, John B. Buse, Zhen Gu*

*Corresponding author. Email: guzhen@ucla.edu

Published 10 July 2019, *Sci. Adv.* **5**, eaaw4357 (2019)
DOI: 10.1126/sciadv.aaw4357

This PDF file includes:

- Scheme S1. Synthesis route of polymers.
- Fig. S1. Characterization of the complex.
- Fig. S2. ¹H NMR spectra of various compounds synthesized.
- Fig. S3. In vitro insulin release studies.
- Fig. S4. Evaluation of insulin complexes in type 1 diabetic mice.
- Fig. S5. Host response and toxicity evaluation in diabetic mice.
- Fig. S6. The Masson's trichrome staining sections of the skin with or without treatment.
- Fig. S7. The immunofluorescence staining sections of the skin with or without treatment.
- Fig. S8 Characterization of MN array patch.
- Fig. S9. Glucose challenge study in diabetic minipigs.
- Table S1. The BGLs of diabetic pigs.



Scheme S1. Synthesis route of polymers.

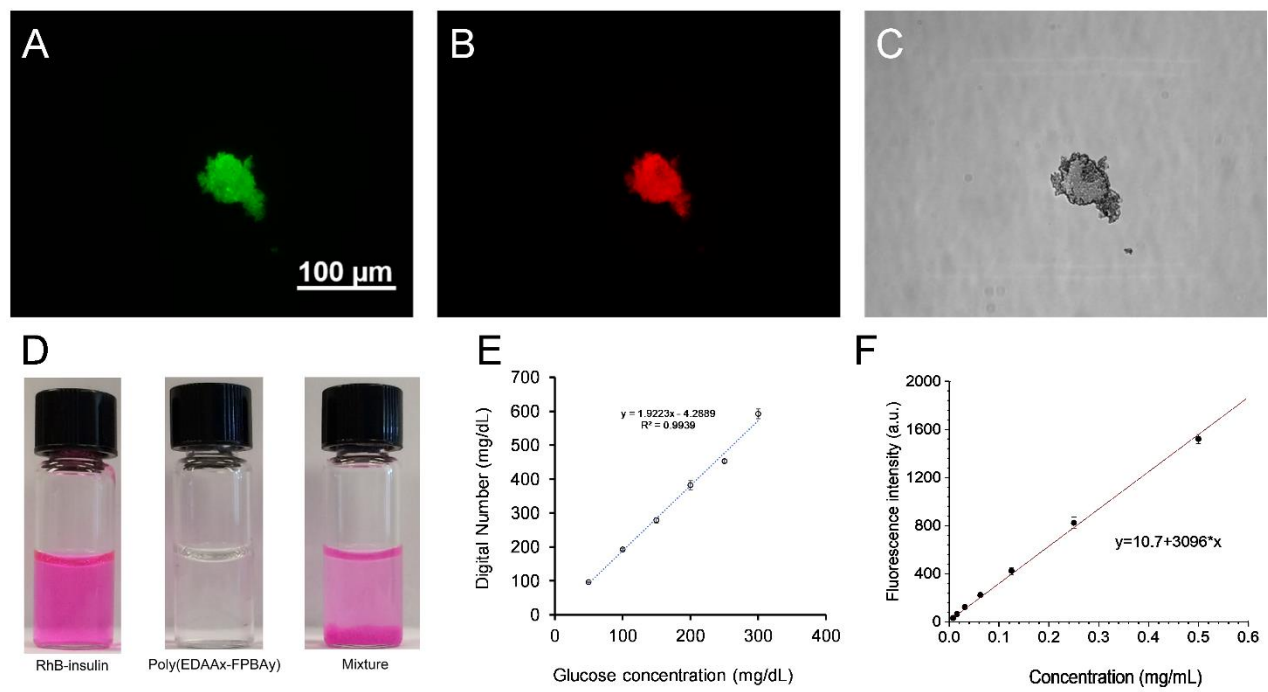


Fig. S1. Characterization of the complex. (A-C) Representative images of the insulin-polymer complex. (A) FITC-labeled poly(EDAA_{0.4}-FPBA_{0.6}) is shown in green; (B) Rhodamine B-labeled insulin is shown in red; (C) bright field image. (D) Representative images of solutions containing RhB-insulin, Poly(EDAA_{0.4}-FPBA_{0.6}) and their mixture after adjusting pH to 7.4. (E) The standard curve of glucose concentration in PBS 7.4. The glucose concentration was measured using a blood glucose meter (Clarity Plus). Error bars represent S.D. ($n=3$). (F) The fluorescence intensity of RhB-insulin as a function of concentration.

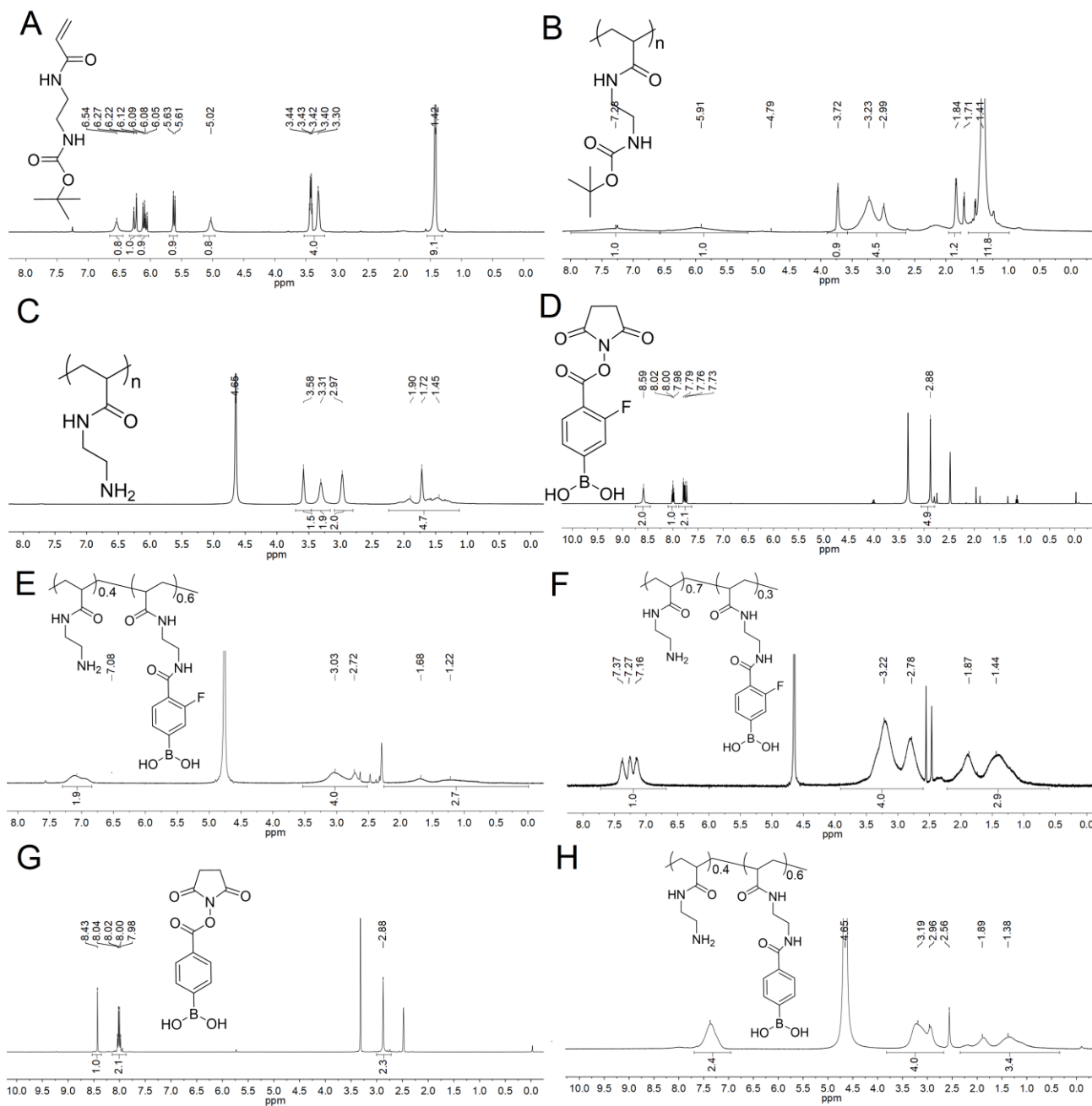


Fig. S2. ¹H NMR spectra of various compounds synthesized. (A) ¹H-NMR spectrum of Boc-EDAA in CDCl₃. (B) ¹H-NMR spectrum of poly(Boc-EDAA) in CDCl₃. (C) ¹H-NMR spectrum of poly(EDAA) in D₂O. (D) ¹H-NMR spectrum of FPBA-NHS in DMSO-d₆. (E) ¹H-NMR spectrum of poly(EDAA_{0.4}-FPBA_{0.6}) in acidic D₂O. (F) ¹H-NMR spectrum of poly(EDAA_{0.7}-FPBA_{0.3}) in acidic D₂O. (G) ¹H NMR spectrum of PBA-NHS in DMSO-d₆. (H) ¹H-NMR spectrum of poly(EDAA_{0.4}-PBA_{0.6}) in acidic D₂O.

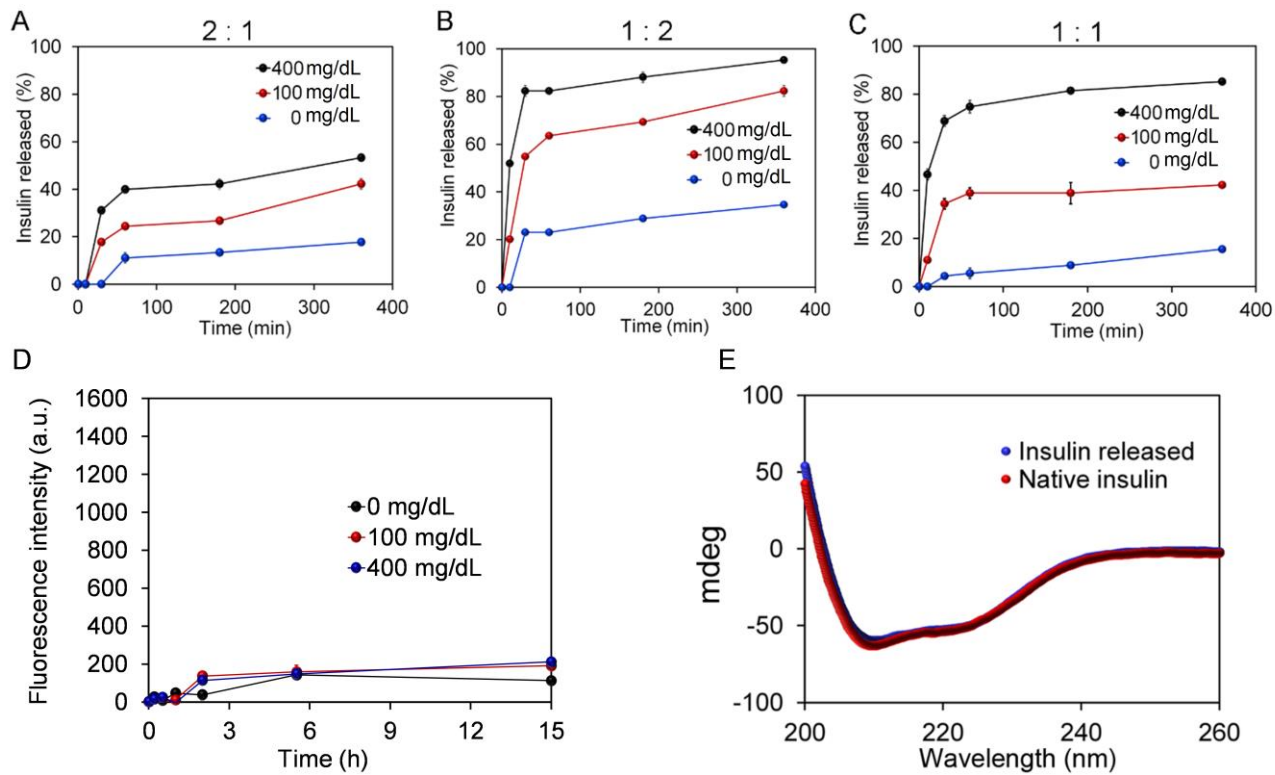


Fig. S3. In vitro insulin release studies. (A-C) Insulin release from the complexes prepared from poly(EDAA_{0.4}-FPBA_{0.6}) and insulin with different weight ratios of poly(EDAA_{0.4}-FPBA_{0.6}) to insulin. Data are shown as mean \pm S.D. ($n=3$). (D) The fluorescence intensity of the supernatant as a function of glucose concentration over time. The complex was prepared from an equal weight of insulin and poly(EDAA_{0.7}-FPBA_{0.3}). Data are shown as mean \pm S.D. ($n=3$). (E) Circular dichroism spectra of native insulin solution (0.5 mg/mL) and insulin released from F-insulin (0.5 mg/mL).

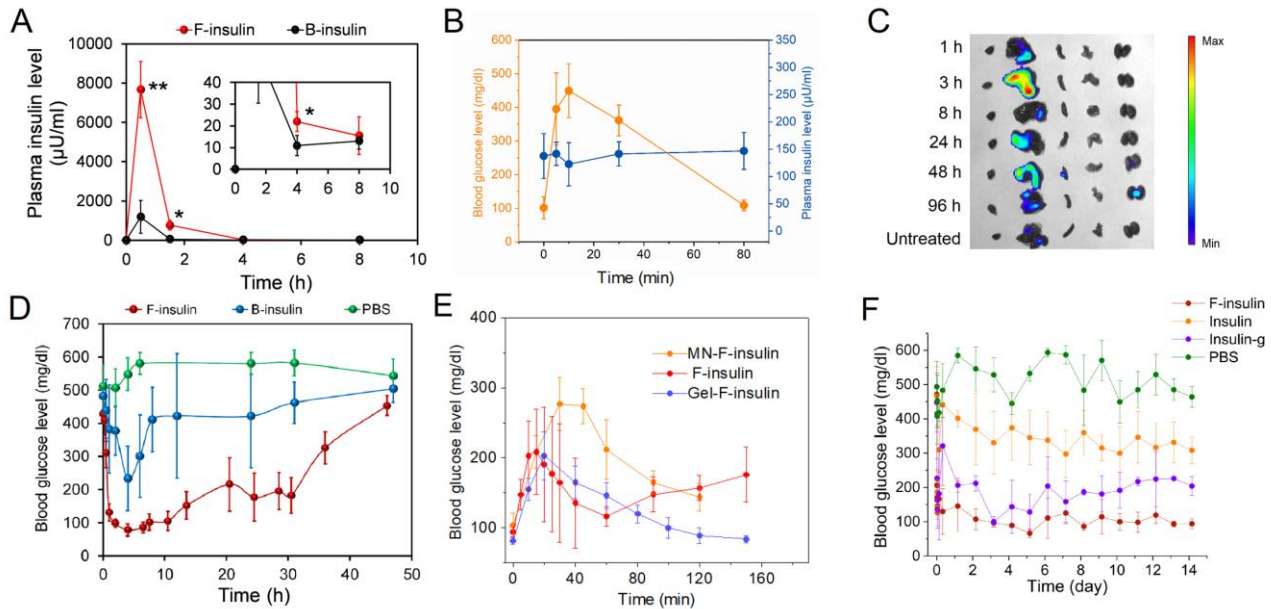


Fig. S4. Evaluation of insulin complexes in type 1 diabetic mice. (A) The plasma insulin levels in type 1 diabetic mice treated with F-insulin or B-insulin. Data are shown as mean \pm S.D. ($n=3$). Statistical significance was calculated *via* Student's t-test. Inset: the data at 2 hours post-treatment. $*P < 0.05$, $**P < 0.01$. (B) Change of plasma insulin glargine level after intraperitoneal glucose challenge. The glucose was given at 4-hours post-treatment of insulin-glargine at a dose of 80 U/kg. Data are shown as mean \pm S.D. ($n=5$). (C) The biodistribution of the polymer after subcutaneous injection of F-insulin. Poly(EDAA_{0.4}-FPBA_{0.6}) was labeled with Cy5. From left to right: heart, liver, spleen, lung, and kidney. (D) Blood glucose levels of diabetic mice treated with subcutaneous injection of F-insulin loaded PF-127 gel. The dose was set as 300 U/kg. Data are presented as mean \pm S.D. ($n=5$). (E) IPGTT at three-hour post-treatment of F-insulin loaded in PF-127 gel. The insulin dose was set as 300 U/kg. Glucose was given at 1.5 g/kg. The results of F-insulin (from Fig. 4D) and MN-F-insulin (from fig. S8B) were also incorporated for comparison. Data are presented as mean \pm S.D. ($n=5$). (F) The blood glucose levels of diabetic mice treated with F-insulin, insulin glargine (insulin-g), and human recombinant insulin (insulin). The group treated with PBS was used as a control. The diabetic mice received two injections each day, with a single dose of 80 U/kg. The blood glucose levels were measured after four hours from the first treatment each day. Data are presented as mean \pm S.D. ($n=4$).

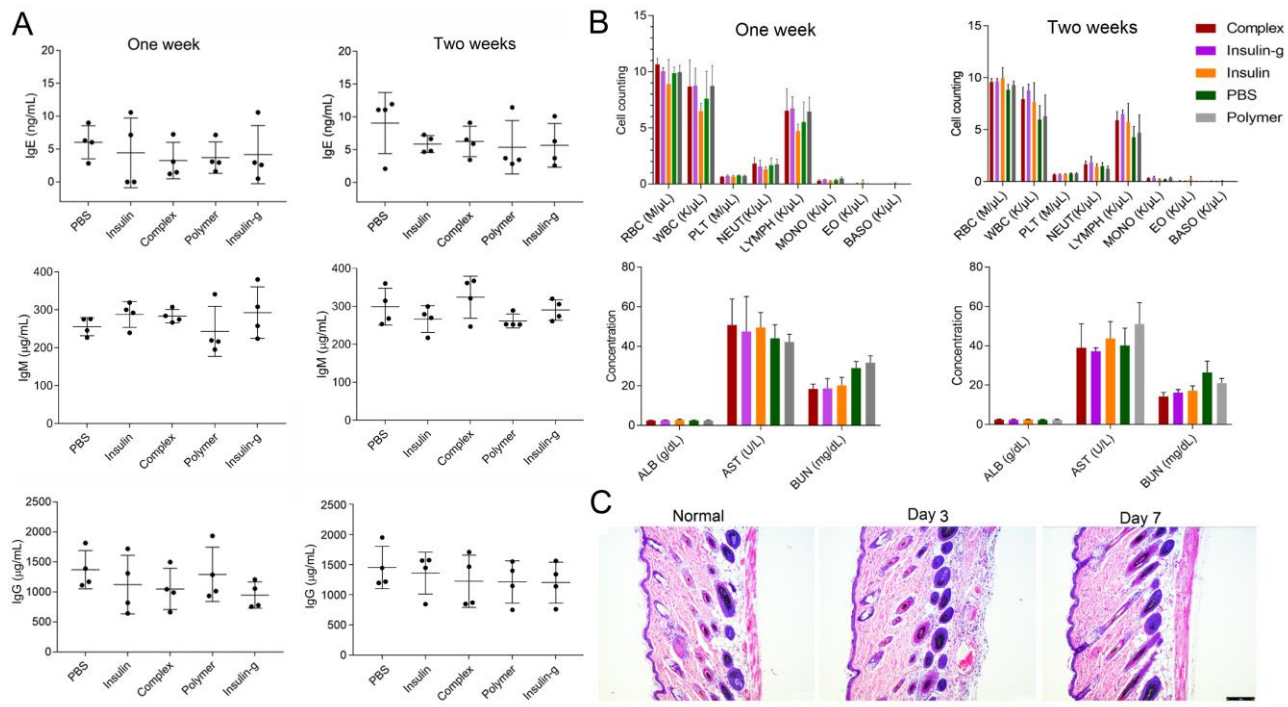


Fig. S5. Host response and toxicity evaluation in diabetic mice. (A) IgE, IgM and IgG levels following one- or two-week-long treatment of native insulin, complex (F-insulin), poly(EDAA_{0.4}-FPBA_{0.6}) (polymer) or insulin glargine (insulin-g). The group treated with PBS was used as a control. The dose was set as 80 U/kg. Each mouse received two injections every day. The serum was obtained after one- or two-week treatment. IgE, IgM and IgG levels in serum were detected using ELISA. Data are presented as mean \pm S.D. ($n=4$). (B) Complete blood counts, and ALB, AST and BUN levels of the diabetic mice after various treatments. The blood was obtained from diabetic mice treated with various formulations after continuous treatment for one or two weeks. The insulin-equivalent dose was 80 U/kg. Each mouse received two treatment every day. Red blood cell, RBC; white blood cell, WBC; platelet, PLT; neutrophil, NEUT; lymphocyte, LYMPH; monocyte, MONO; eosinophil, EO; basophil, BASO; albumin, ALB; Aspartate aminotransferase, AST; blood urea nitrogen, BUN. Data are presented as mean \pm S.D. ($n=4$). (C) H&E-stained section of mouse skin treated with PF-127 gel loaded with F-insulin. Scale bar, 75 μ m.

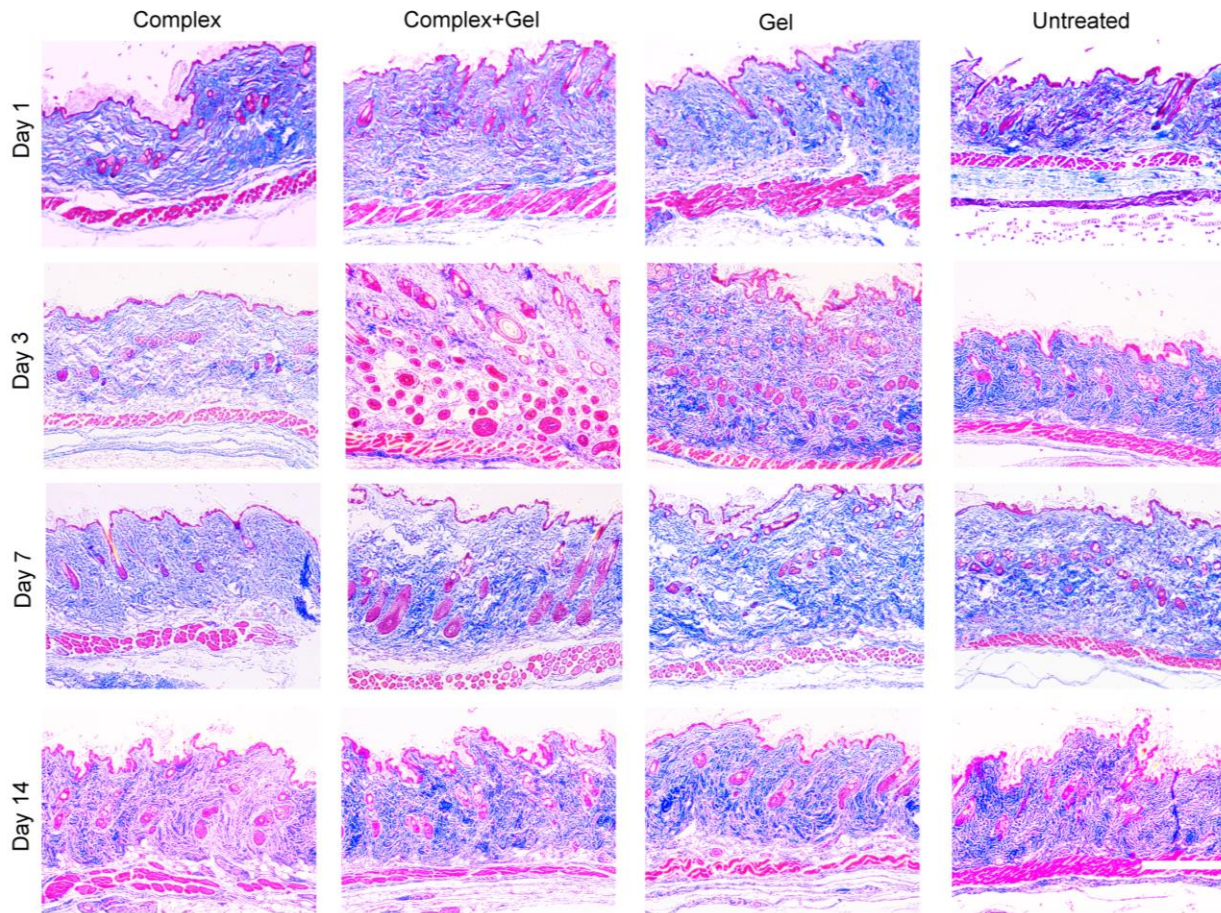


Fig. S6. The Masson's trichrome staining sections of the skin with or without treatment. The skin was obtained on day 1, 3, 7 or 14 post-treatment. The skin without treatment was used as the control. Scale bar, 300 μm .

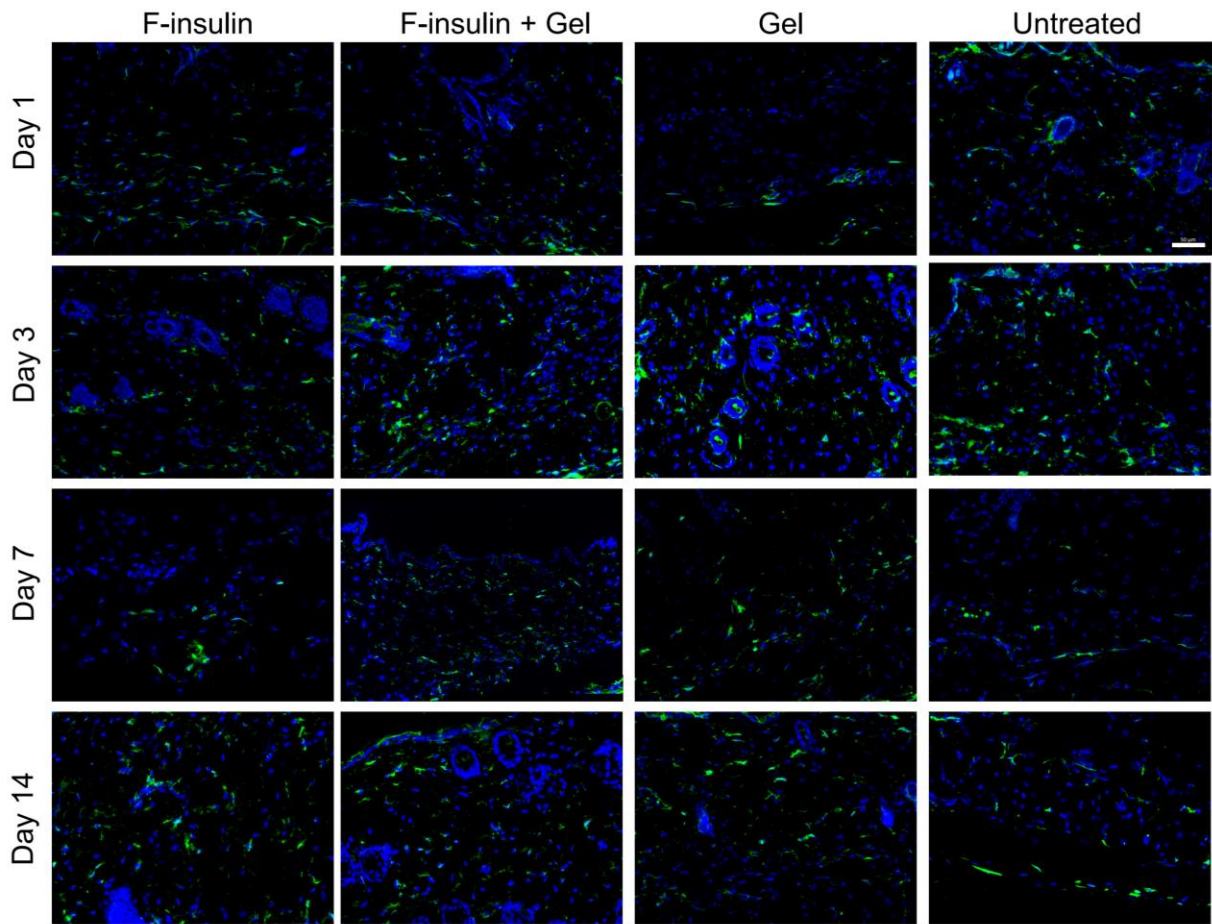


Fig. S7. The immunofluorescence staining sections of the skin with or without treatment. The skin was obtained on day 1, 3, 7 or 14 post-treatment. The skin without treatment was used as the control. The pan-macrophage marker F4/80 (green) was used for identifying the macrophages. The nuclei were stained with DAPI and shown in blue. Scale bar, 50 μm .

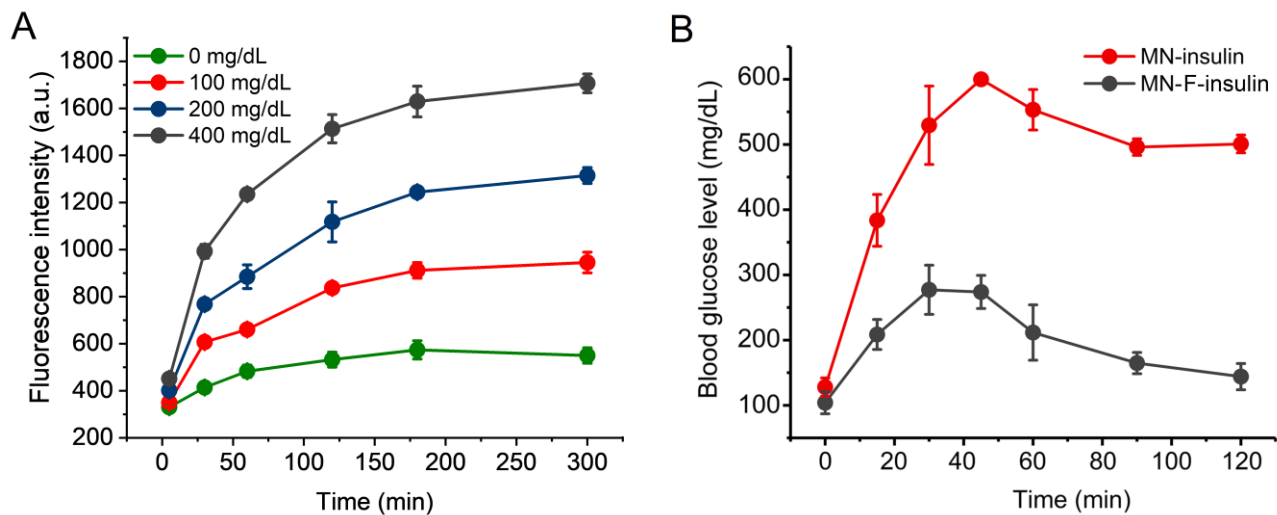


Fig. S8. Characterization of MN array patch. (A) Fluorescence intensity of the released RhB-insulin from F-insulin loaded in microneedle array patch as a function of time and glucose concentration. Data are shown as mean \pm S.D. ($n=3$). (B) *In vivo* glucose tolerance test of diabetic mice. The glucose was given three hours post-treatment with MN-insulin or MN-F-insulin at 1.5 g/kg. Data are shown as mean \pm S.D. ($n=5$).

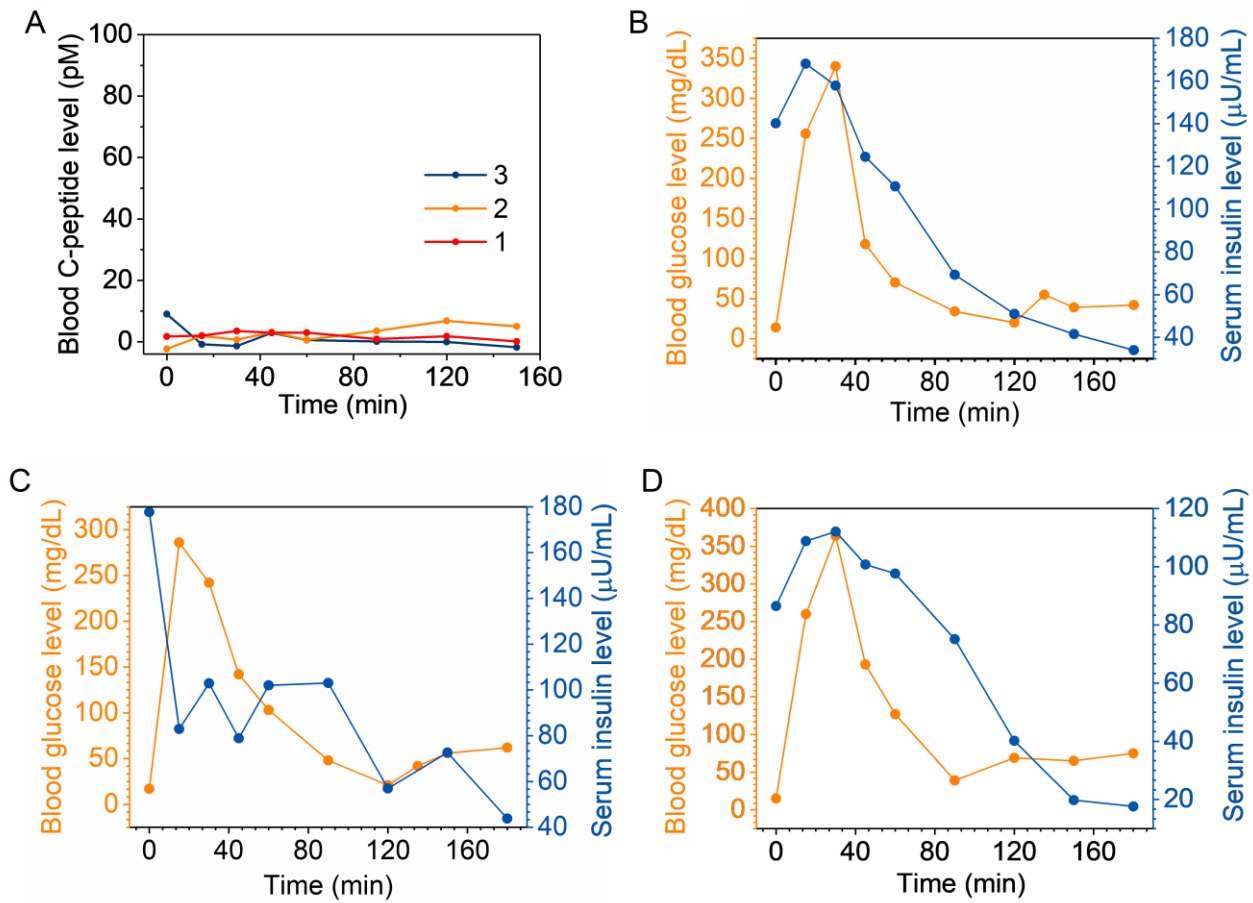


Fig. S9. Glucose challenge study in diabetic minipigs. (A) *In vivo* glucose tolerance test of diabetic minipigs at four hours post-treatment of F-insulin at a dose of 1 U/kg. Three pigs in total were used in this study. The C-peptide was monitored using a Porcine C-peptide ELISA (Mercodia). (B-D) *In vivo* glucose tolerance test in diabetic minipigs at four hours post-treatment of free insulin at a dose of 1 U/kg. Dextrose solution (5%) was intravenously infused at a dose of 0.75 g/kg. The rate of infusion was set as 1 L/h. panels B, C, and D indicates pig 1, 2 and 3, respectively.

Table S1. The BGLs of diabetic pigs.

Treatment	Time (h)	Blood glucose (mg/dL)
1-insulin	3.5	41
1-F-insulin	3	44
1-F-insulin	5	47
2-insulin	3.5	38
2-insulin	5	42
2-F-insulin	3.5	51
3-insulin	4	37
3-insulin	5	36
3-insulin	6	47
3-F-insulin	5.5	43
3-F-insulin	7	54